PHYSICAL REVIEW B VOLUME 49, NUMBER 7 15 FEBRUARY 1994-I

Competition between miniband conduction and intervalley transfer in $GaAs/Ga_{1-x}Al_xAs$ superlattice oscillators investigated by hydrostatic pressure

E. Dutisseuil, A. Sibille,* and J. F. Palmier
France Telecom/Centre National d'Etudes des Télécommunications/PAB, 196 avenue Henri-Ravera, Boîte Postale 107, 92220 Bagneux Cedex, France

F. Aristone
Centre National de la Recherche Scientifique, Institut National des Sciences Appliquées, Laboratoire de Physique des Solides, avenue de Rangueil, 31077 Toulouse Cedex, France and Centre National de la Recherche Scientifique, Service National des Champs Intenses 25, avenue des Martyrs, 38042 Grenoble, France

F. Mollot
Institut d'Electronique et Microélectronique du Nord, Université des Sciences et Technologies de Lille, 59655 Villeneuve d'Ascq Cedex, France

V. Thierry-Mieg
Centre National de la Recherche Scientifique, Laboratoire de Microélectronique et Microstructure, 196 avenue Henri-Ravera, 92220 Bagneux Cedex, France

(Received 4 October 1993; revised manuscript received 15 November 1993)

We investigate experimentally hot-electron transport in $GaAs/Ga_{0.5}Al_{0.5}As$ superlattice (SL) oscillators designed for high-frequency operation at room temperature. Two effects are considered: intraminiband heating and intervalley scattering involving L and X well and barrier states. We show that both effects can be sensitively measured by using the hydrostatic-pressure dependence of the SL electrical conduction. Finally we demonstrate the feasibility of wide-miniband ultrafast $GaAs/Ga_{1-x}Al_xAs$ SL transport, fully devoid of intervalley transfer.

In 1970, Esaki and Tsu brought about the idea that negative differential conductance (NDC) might be obtained in superlattices (SL's).[1] Most theories developed up to now rely on semiclassical approximations based on the Boltzmann transport equation (BTE),[2] although some authors have incorporated quantum effects through a Wigner formulation.[3] As a matter of interest, the two basic effects pertaining to miniband NDC in SL are (i) negative miniband effective mass along k_z beyond $\pi/2d$ (d being the SL period), (ii) Bloch oscillations for Bragg-statted electrons beyond π/d. Both effects have been calculated and partly involved in the NDC.[4] Experimentally, however, the first clear observation of NDC as a SL effect was due to space charge effects and high field domain formation in highly doped sample.[5] It was not until 1989 (Refs. 6 and 7) that systematic and reproductible investigation demonstrated the occurrence of miniband NDC as proposed by Esaki and Tsu.

It has been shown that the NDC could be at the origin of instabilities such as commonly known in the Gunn effect and therefore, exploitable for high-frequency oscillator applications.[8,9] All these features are clearly unrelated to intervalley transfer, which is consequently a detrimental effect to be avoided as much as possible.

In this work we address this competition in $GaAs/Ga_{0.5}Al_{0.5}As$ superlattices, specially designed to operate as millimeter wave oscillators, by measuring the hydrostatic pressure dependence of the SL current-voltage characteristics. The experimental data are compared to our numerical simulations of transport which supply the velocity versus field $V(F)$ laws by solving the BTE. The computations incorporate the main realistic scattering mechanisms, namely, optical- and acoustic-phonon scattering, interface roughness fluctuation scattering, and ionized impurity scattering.

The two samples used in this study have been grown by molecular-beam epitaxy on Si-doped (001) GaAs substrates and basically consist of 0.5-μm Si-doped (10^{17} cm^{-3}) SL under study sandwiched between n^+ contacts, through n^+ SL intermediate layers of graded parameters intended to facilitate electron injection. The SL nominal parameters are (19/4) (19 monolayers of GaAs/4 monolayers of $Ga_{0.5}Al_{0.5}As$) for the first sample and (17/3) for the second one. These choices offer ground-state conduction miniband width Δ of $\Delta_{(19/4)}=70$ meV and $\Delta_{(17/3)}=113$ meV, as calculated by envelope function approximation using $\mathbf{k}\cdot\mathbf{p}$ derived effective masses. Conventional lithographic techniques were employed to provide top and bottom AuGe Ohmic contacts and etched mesas. Current measurements under hydrostatic pressure were performed using liquid pressure cell techniques at room temperature and pressures were measured by means of a calibrated InSb resistance. In the following we specifically focus on SL (19/4), as qualitatively identical results were obtained on SL (17/3).

The band structure of SL (19/4) is schematically illus-

trated in Fig. 1. It consists of (in increasing energy) the Γ-related conduction miniband (Γ^c), the first Γ excited miniband (Γ^1), the lowest L band, and the first X_z and X_{xy} bands.[10] They provide energy (ε) offsets (in units of miniband width Δ) of $\varepsilon(\Gamma^1)-\varepsilon(\Gamma^c_{\text{bottom}})=3.3$ for (19/4) and 2.4 for (17/3) $\varepsilon(L)-\varepsilon(\Gamma^c_{\text{bottom}})=3.5$ and 2.2, respectively, and $\varepsilon(X)-\varepsilon(\Gamma^c_{\text{bottom}})>5.4$ and 3.5, respectively, whose rates were expected to express sufficiently high satellite valleys compared to the conduction miniband Γ to dismiss any thermal population. Indeed, our BTE simulations predict a mean electronic energy of about 1.5Δ at the critical field F_c for the onset of NDC.

We present in Fig. 2(a) current-voltage $I(V)$ measurements at 300 K and 1 bar for both SL's. They exhibit the required NDC for oscillator applications beyond 0.6 V [for SL (19/4)] and 0.5 V [for SL (17/3)]. The fairly good uniformity of the electric field in these relatively highly doped SL's allows a reliable comparison between data and our $V(F)$ simulations (described below), for fields lower than F_c. We thus determine the latter to be 4.2 and 3.8 kV/cm, respectively, in both samples, taking into account a series resistance of 5 Ω.

Current-pressure $I(P)$ measurements of the SL (19/4) under pressures ranging from 1 bar to 10 kbar are shown in Fig. 2(b) at different biases up to $\frac{2}{3}$ of the critical voltage. A quasilinearity can be observed for each applied bias below approximately 4 kbar, while a superlinearity appears above. It is therefore apparent that two different mechanisms are operating as regards the sensitivity of the device conductance with pressure, whether low or high hydrostatic pressures. This conclusion is very clearly confirmed by the voltage dependence of the pressure coefficient of current $(1/I)(dI/dP)$ in these two [i.e., low (LPR) and high (HPR)] pressure regimes, as shown in Figs. 3(a) and 3(b) (full lines): we observe a *decrease* of this coefficient with bias under low pressure, while an *increase* is found under high pressure. We now show that an excellent explanation of these two regimes can be related to the pressure dependence of the SL band structure and electronic heating.

One first effect (*intravalley*) which occurs at any pressure is the increase of the electron effective mass, both in the well and barrier materials. The resulted shrinking of the miniband width will reduce the perpendicular electron velocity and therefore SL conduction in a predictable way.

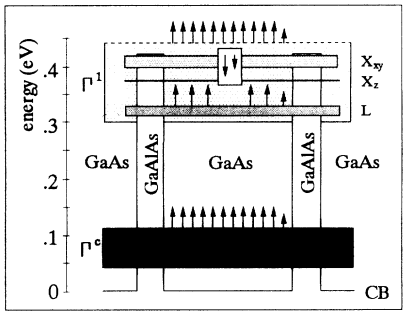

FIG. 1. Schematic band diagram of the (19/4) SL. Vertical arrows schematize direction and value of band shifting under pressure.

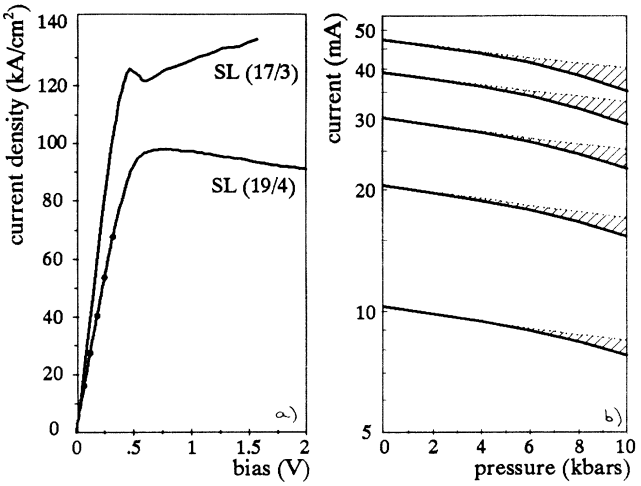

FIG. 2. (a) Current-voltage characteristics for both SL's at 300 K and 1 bar. (b) Current-pressure characteristics for the (19/4) SL (full lines). Dashed lines are the intravalley effect; hatches, the difference which is ascribed to the intervalley effect.

The second effect (*intervalley*) should be ascribed to the pressure-induced reduction of energy interval between the main Γ conduction miniband and the minibands derived from X and L satellite minima. Because of this reduction, some electrons will be thermally transferred from the Γ miniband to these satellite minibands characterized by low mobilities, thereby further reducing the net SL conductance (intervalley transfer).

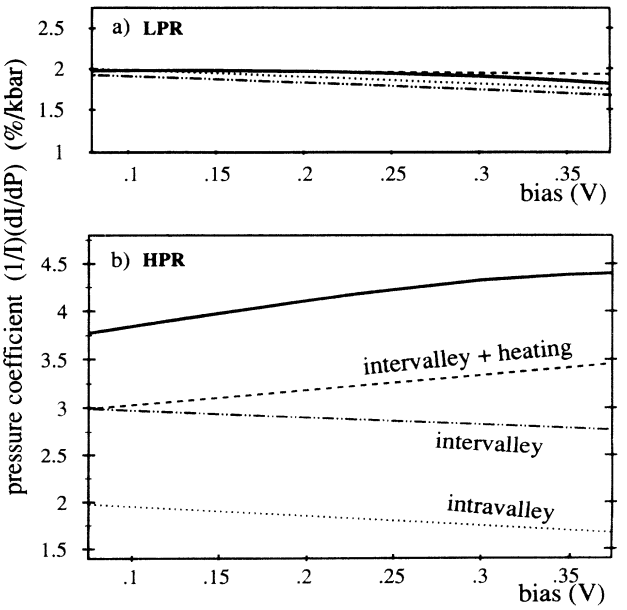

FIG. 3. Pressure coefficient as a function of bias in the low [between 0 and 2 kbar, (a)] and high [between 8 and 10 kbar, (b)] pressure regimes: experiment, ——; simulation of intravalley effect alone, · · · ·; the same with intervalley effect added: –··–··–··, without electronic temperature and — — —, with electronic temperatures.

In order to confirm these speculations, we now compare our experimental data with calculations of the SL conductance taking into account both of these effects. The *intravalley* effect was straightforwardly accounted for by simulating the pressure-dependent $V(F)$ through pressure-dependent effective masses with a pressure coefficient of $(1/m^*)(dm^*/dP)$ allowed for in the calculation of the Γ-related miniband of conduction. Our simulations indeed predict a decreasing electron velocity with increasing pressure as expected. Moreover, a particularly interesting result is the lesser effect of pressure when the bias is increased, exactly along with our experimental observations in the LPR [see Fig. 3(a) in dotted lines]. The *intervalley* effect [emphasized by hatches in Fig. 2(b)] has been evaluated by a simple calculation of the electronic population in each miniband. This has been achieved by considering the energy gaps between each of these minibands, their SL type density of states (depending on the parallel effective masses) and the electronic statistic distribution (assumed quasi-Maxwellian in parallel directions). The following data were used in wells (w) and barriers (b).[11]

For w (GaAs),

$m^*_{L_{\text{perp}}}=0.11$ (for confinement),

$m^*_{L_\parallel}=0.0754$ and 1.29 (for density of states),[12]

For b ($Ga_{0.5}Al_{0.5}As$),

$m^*_\Gamma=0.1085$, $m^*_{(X_t)}=0.2$, $m^*_{(X_l)}=1.2$,

$m^*_L=0.14$ (for confinement),

$m^*_{L_\parallel}=0.0964$ and 1.3 (for density of state).[12]

Energy offsets of bulk materials:[11] $\varepsilon^w_L-\varepsilon^w_\Gamma=0.284$ eV and $\varepsilon^b_X-\varepsilon^w_\Gamma=0.37$ eV (to which confinement and strain must be added) and pressure coefficient of band gaps:

$d\Delta^\Gamma_g/dP=11.5$ meV/kbar (Ref. 11),

$d\Delta^L_g/dP=5.5$ meV/kbar (Ref. 13),

$d\Delta^X_g/dP=-1.5$ meV/kbar (Ref. 13).

At room temperature, we have calculated the total population of the upper valleys (which depends on the parallel masses and multiplicity of each valley) to be definitely less than 0.5% at room pressure and less than 5% at 10 kbar. The pressure coefficients of transferred electrons have then been calculated on the whole pressure range (0–10 kbar) and taken into account in the simulation of the intravalley effect. The best fit of experimental data has been achieved with a pressure coefficient of intravalley effect $(1/m^*)(dm^*/dP)=0.70\%$/kbar (identical in well and barrier). This value is in excellent agreement with those available in the literature [0.68%/kbar (Ref. 14) (calc.), 0.70%/kbar (Refs. 15 and 16) (expt.)]. The simulated intravalley effect alone and the same added with electron transfer are presented in Fig. 3 in dotted lines [and also in Fig. 2(b)] and dashed lines, respectively.

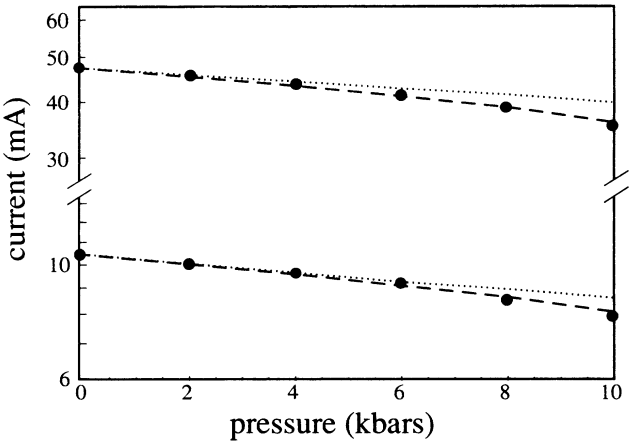

FIG. 4. Current as a function of pressure for the lowest and for the highest voltage (experiment, ● ● ●; simulation of intravalley effect alone, · · · ·; the same with intervalley effect added, — — —).

A good agreement is found in the LPR but in the high-pressure one, HPR, a qualitative agreement is not yet achieved because no increased pressure coefficient $(1/I)(dI/dP)$ with bias is found. The reason is that *we have to take into account a moderate electronic heating* (about 58 K at 375 mV in the HPR) which is inherent to nonlinear miniband transport as long as Δ appreciably exceeds k_BT.[17] Indeed, our BTE calculations predict a spreading of the quasi-Maxwellian parallel distribution (with an equivalent electronic temperature T_e) due to the redistribution of energy acquired during the perpendicular electronic acceleration under applied electric field. For instance, 350 K are directly yielded at room temperature for the higher explored voltage (corresponding to $\frac{2}{3}$ of the critical field F_c). As a consequence, the thermal transfer of electrons to the upper satellite valleys is increased not only when pressure is increased but also when bias is increased.

Finally the calculation of the pressure coefficient $(1/I)(dI/dP)$ takes into account *intravalley* effect and pressure and bias-dependent *intervalley* effect; we present the results in Fig. 3 (dotted lines). Now the two pressure regimes are found again. Moreover, we can say that a satisfactory quantitative agreement is obtained considering the precision imposed by these two figures: Indeed, the maximum discrepancy in current-pressure $I(P)$ (Fig. 4) stands below 2% in the whole pressure and voltage ranges explored. A possible deviation of the SL parameters from the nominal ones may explain the small quantitative discrepancy observed for intervalley effect in the HPR.

In conclusion, we have demonstrated a negligible intervalley transfer at room temperature and pressure as well as the presence of electronic heating in the perpendicular conduction of $GaAs/Ga_{0.5}Al_{0.5}As$ superlattices, by means of pressure esxperiments. A satisfactory agreement has been obtained between calculated electronic temperatures T_e and those which are necessary to explain

the experimental bias and pressure dependences of currents.

From these results, we can safely conclude that the investigated millimeter-wave SL oscillators are negligibly affected by intervalley transfer at room temperature. Therefore it clearly appears that a comfortable margin is assured in the design of ultrahigh frequency GaAs/$Ga_{1-x}Al_xAs$ SL oscillators based on single miniband Esaki-Tsu NDC.

The authors would like to express their gratefulness to S. Vuye and J. C. Esnault for help in sample processing, B. Goutiers for taking part in pressure measurements, and J. C. Portal for hospitality in his laboratory.

---

*Also at ENSTA, 32 bd Victor 75015 Paris, France.

[1]L. Esaki and R. Tsu, IBM J. Res. Dev. **14**, 61 (1970).

[2]See, e.g., M. Artaki and K. Hess, Superlatt. Microstruct. **1**, 489 (1985) or X. L. Lei, N. J. M. Horing, and H. L. Cui, Phys. Rev. Lett. **66**, 3277 (1991); J. F. Palmier. G. Etemadi, A. Sibille, M. Hadjazi, F. Molot, and R. Planel, Surf. Sci. **267**, 574 (1992).

[3]P. J. Price, IBM J. Res. Dev. **17**, 39 (1973); R. K. Reich and D. K. Ferry, Phys. Lett. **91A**, 31 (1992).

[4]A. Sibille, J. F. Palmier, M. Hadjazi, H. Wang, and F. Mollot, in 21st ICPS, Beijing, 1992, edited by Ping Jiang and Hou-Zhi Zheng (World Scientific, Beijing, 1992).

[5]L. Esaki and L. L. Chang, Phys. Rev. Lett. **33**, 495 (1974).

[6]A. Sibille, J. F. Palmier, C. Minot, and F. Mollot, Appl. Phys. Lett. **54**, 165 (1989).

[7]A. Sibille, J. F. Palmier, F. Mollot, E. Wang, and J. C. Esnault, Phys. Rev. B **39**, 6272 (1989).

[8]M. Hadjazi, J. F. Palmier, A. Sibille, H. Wang, E. Paris, and F. Mollot, Electron. Lett. **29**, 648 (1993).

[9]H. Le Person, C. Minot, L. Boni, J. F. Palmier, and F. Mollot, Appl. Phys. Lett. **60**, 11 (1992).

[10]Owing to confinement and strain, the valley degeneracy between X minima along z (growth axis) and x,y directions is lifted.

[11]S. Adashi, J. Appl. Phys. **58**, 3 (1985).

[12]Masses for L valley are calculated using the formula $m^*_{perp}=m_{(001)}=(3m^*_{long}m^*_{trans})/(m^*_{trans}+2m^*_{long})$ and $m^*_{\|}$ =masses in plane$=(2m^*_{long}+m^*_{trans})/3$ and m^*_{trans} [see F. Stern and W. E. Howard, Phys. Rev. **163**, 3 (1967)].

[13]E. E. Mendez, E. Calleja, and W. I. Wang, Phys. Rev. B **34**, 8 (1986).

[14]N. E. Christensen, Phys. Rev. B **30**, 5733 (1984), and references therein.

[15]P. Lefebvre, B. Gil, and H. Mathieu, Phys. Rev. B **35**, 11 (1987).

[16]G. D. Pitt, J. Lees, R. A. Hoult, and R. A. Stradling, J. Phys. C **6**, 3282 (1973).

[17]I. B. Levinson and Ya. Yasevichyute, Zh. Eksp. Teor. Fiz. **62**, 1902 (1972) [Sov. Phys. JETP **35**, 991 (1972)].

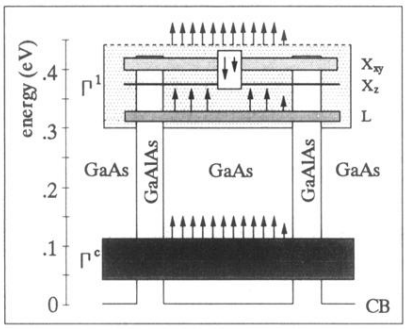

FIG. 1. Schematic band diagram of the (19/4) SL. Vertical arrows schematize direction and value of band shifting under pressure.